

Stress Analysis of Uniform Circular Cylindrical Shells with Large Circular Holes

Rishicca Kamalarajah, William Stoffberg, John W. Bull, Mahmoud Chizari

Abstract— a finite element analysis of a uniform cylindrical shell with a large circular cut-out is presented. In this analysis three hole sizes are considered, respectively with radius a A = 62.87 mm; a B = 126.49 mm; a C = 196.01 mm. For the purpose of the research, the computer aided engineering software Abaqus (Dassault Systèmes, FR) is adopted in order to simulate material behaviour under compressive and torsional loading. The investigation is carried out with respect to the elastic behaviour of the material.

Index Terms— finite element analysis, Abaqus, cylindrical shells, stress concentration, circular holes, torsion, compression

I. INTRODUCTION

THIN-walled structures in the form of shells are common design elements used in many branches of applied sciences such as civil, mechanical, aerospace, marine, and petrochemical engineering [1]. In a relatively large number of situations, the shell structure may experience a modification of its geometry through circular cut-outs on the surface, compromising the axial symmetry of the stress distribution and considerably altering the stress from that of the uncut shell [2]. Typical examples of perforated shells include piping connections, electrical systems and aircrafts fuselages [3]. The determination of the stress concentration around large circular holes are of particular interest during the shell's structural design [4] as these types of structure are subjected to loading of various types which may cause deformation and cracking initiation [2].

John Bull [5] in his previous works on circular holes in cylindrical shells proposed an experimental examination of the problem through a series of tests on three pipes with different hole sizes, namely $\mu = 2.037, 4.084$ and 6.344 (where $\mu = \{[12(1-\gamma^2)]^{0.25}/2\} \times [a/(Rt)^{0.5}]$, see Table 1 for the list of abbreviations) for loading of axial compression, torsion and three point bending. In previous literature, a theoretical analysis using the finite element method was

Manuscript received March 17, 2015; revised March 31, 2015.

Rishicca Kamalarajah is with Mechanical, Aerospace and Civil Engineering Department, College of Engineering, Design and Physical Sciences, Brunel University London, UK. Email: r.kamalarajah@gmail.com

William Stoffberg is with Mechanical, Aerospace and Civil Engineering Department, College of Engineering, Design and Physical Sciences, Brunel University London, UK. Email: wstoffberg@hotmail.com

John W. Bull is with Mechanical, Aerospace and Civil Engineering Department, College of Engineering, Design and Physical Sciences, Brunel University London, UK. Email: john.bull@brunel.ac.uk

Mahmoud Chizari (corresponding author) is with Mechanical, Aerospace and Civil Engineering Department, College of Engineering, Design and Physical Sciences, Brunel University London, Uxbridge, UB8 3PH, UK. Fax: +44 1895256392, E-mail: mahmoudchizari@yahoo.com

adopted [5] to obtain the stresses that would occur in pipes with the same dimension, boundary conditions, and loadings as those tested experimentally. In more recent studies, different approaches have been tested to determine the curvature effects on the stress concentration, but published papers are not widely available on the numerical study with the finite element software Abaqus on the elastic behaviour of shells under external loading [4].

This paper, thus, seeks the validation of the computer aided software Abaqus in simulating Bull's experiment [5],

TABLE I
GEOMETRIC PROPERTIES

Symbol	Quantity
a	Radius of the hole in the pipe
E	Young's modulus
R	Radius of the middle surface of the pipe
t	Pipe thickness
γ	Poisson's ratio
ϕ	Angle around hole in the pipe
μ	$\{[12(1-\gamma^2)]^{0.25}/2\} \times [a/(Rt)^{0.5}]$

and hence to compare the results.

II. METHODS

A. Shell Model

In his study on the linear elastic theory of thin shells, Gibson points out that the complexity of the problem of large circular holes in cylindrical shell can arise out of the simultaneous presence of two sets of curvature in the same configuration [2]. The pipes in this paper have been modelled following Bull's experiment [5] in which steel cylindrical pipes of $E = 212.414 \text{ kN/mm}^2$ have been employed for the purpose.

The model is a uniform 3D-Deformable-Shell structure of 2000mm length in which three different circular holes of a radius have been cut in the middle of the shell element. The length of the pipe has to be sufficiently long in order to neglect the stresses induced by the hole at the end of the pipe. The geometry of the curvature of the hole has been derived and it is described as follow:

$$y = r_{cylinder} - r_{cylinder} \times \cos\left(\frac{\sqrt{r_{circle}^2 - x^2}}{r_{cylinder}}\right) \quad (1)$$

Due to the elaborated geometry of the structure, many studies have also focused in methods of adapting meshing that significantly influences the quality and accuracy of the

finite element solution, in particular under torsional loading due to the stresses orientation which are not perpendicular to the geometric axis of the shells [6]. Sadowski and Rotter have researched the relationship between mesh and stress field orientation in linear stability analysis of thin shells [7]. In their work, the procedure to generate a well-structured quadrilateral mesh is proposed and it has been proved that the use of quadrilateral and higher order elements give precise and realistic results. Moreover, after a mesh convergence study, the model has been defined by using element S4R: a 4-node doubly curved thin or thick shell, reduced integration, hourglass control, finite element membrane strain for the linear geometric order.

B. Testing procedure

The finite element method has been chosen as an efficient tool of analytical computation in which the mechanical properties of the material (density, Young's Modulus, Poisson's ratio) are taken in account during the performance of the analysis [8]. In this research, Abaqus is being adopted to simulate the elastic behaviour of the shell under different types of applied load.

The properties of the pipes are given in Table 2.

TABLE II
THE THREE STEEL PIPES SPECIFICATIONS

Pipe	Shell Radius [mm]	Thickness [mm]	Hole Radius [mm]	R/t	Poisson's Ratio	E [kN/mm ²]
A	133.50	5.983	62.87	22.65	0.3	212.414
B	133.50	5.983	126.49	22.65	0.3	212.414
C	133.50	5.983	196.01	22.65	0.3	212.414

The material is considered to be uniformly homogeneous, isotropic and perfectly elastic throughout the whole length of the pipe. The yield stress of the metal is 275MPa.

By using the definition of shell element, the thickness of the material has been distributed uniformly at the mid-surface of the pipe in a singly-walled structure. Moreover, the model proposed presents no geometrical imperfections. Through means of assembly, the final configurations of the pipes are as in Figure 1.

A general static procedure has been selected for the analysis, in a full Newtonian solution technique with ramp linear load variation with time. Coupling constraint is defined to provide a rigid constraint between reference nodes, namely RP-1 and RP-2, and the nodes on the circular edge surface. The application of the coupling is to apply kinematic boundary condition and loads to the shell element while defining the end conditions. A completely fixed boundary condition is then created at RP-2. The approximate mesh size for these models was 19, which can be considered as a product of mesh convergence in fine meshes.

The pipes A, B, and C present same features and characteristic, in which forces at RP-1 end are applied and the final design are illustrated as shown in Figures 1, 2, 3.

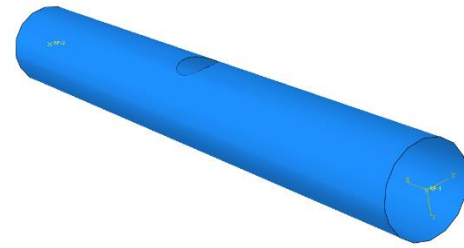


Fig. 1. Finite element model of pipe A with a 125.74 mm diameter hole in middle.

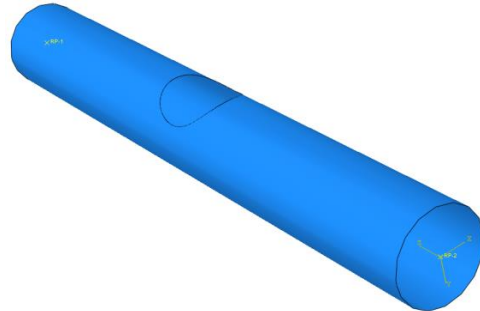


Fig. 2. Finite element model of pipe B with a 252.98 mm diameter hole in middle.

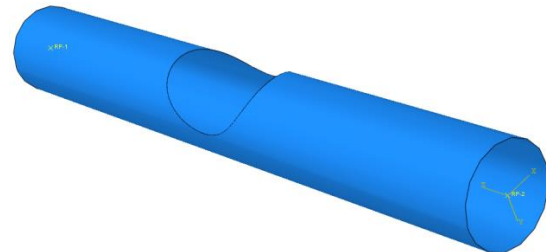


Fig. 3. Finite element model of pipe C with a 392.02 mm diameter hole in middle.

C. Torque Model

A rotation is applied to RP-1 to simulate the effect of torque on the model. The boundary condition at RP-1 is created such that it is fixed in the rotations UR1 (x direction) and UR2 (y direction). A set value to twist is applied in the rotation UR3, which after each analysis is increased incrementally to achieve the range of stress results. The test has been carried out with respect to the yield stress of the steel member; therefore the applied torque is to be small enough to create stresses in the elastic region.

D. Axial Compression Model

An axial force is applied to RP-1 to simulate the effect of axial compression on the model. The boundary condition at RP-1 is created such that it is fixed in the rotations UR1 (x direction), UR2 (y direction) and UR3 (z direction) as well as the translations U1 (x direction) and U2 (y direction). A force of 10,000N applied in the translation U3.

III. RESULTS AND DISCUSSION

A. Axial Compression

The maximum stresses induced by the axial compression were shown to be in two opposite lengths on the circular cut out's edge. These two points lay on the x-axis.

The stresses were compressive in nature and were recorded and the largest of the stresses were recorded for each pipe, the results are shown in Figure 4.

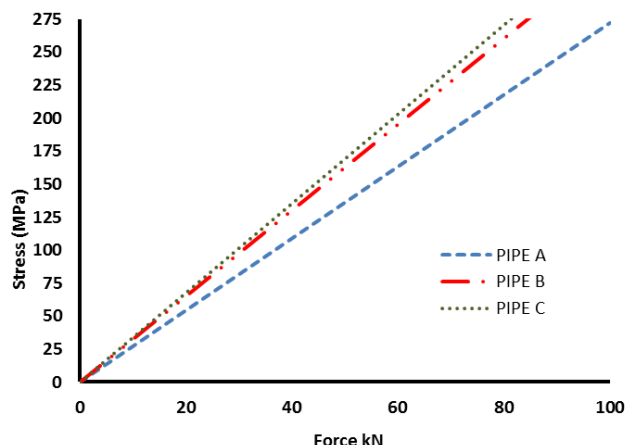


Fig. 4. The result of maximum Mises stress versus axial force applied to the pipes

The analysis results of the three pipes under an axial loading is shown in Figures 5, 6 and 7. As the result shows Pipe C, having the largest stresses of the three. As expected, the larger the hole, the higher the stresses on the pipe. This is down to this pipe being weakened from the loss of structural material.

The pipe under high loading behaves as a hinge at these two points. They buckle outwards, increasing the stress until yield stress is reached. This high stress spreads around the cylinder along the cross section of smallest area. This deformation continues until the circular cut out is 'flattened' and the pipe becomes a hinge in the centre. The image below has been scaled 100 times to display this effect.

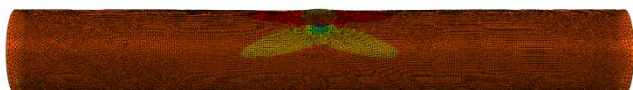


Fig. 5. The results of compressive stress when a compressive axial force applied to pipe A

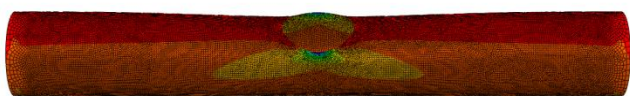


Fig. 6. The results of compressive stress when a compressive axial force applied to pipe B



Fig. 7. The results of compressive stress when a compressive axial force applied to pipe C

The contour legend for Figures 5, 6 and 7 is chromatically distributed having the compression zone with the lowest value of recorded stress along the length of the shell and the highest peaks which are at the edges of the holes.

B. Torsion Loading

The figure above shows the stress around the holes during torsional loading: as it was expected, the maximum stress is obtained in the bottom corners of the holes and interestingly, the yielding stress is reached with a small amount of angular deflection before the pipes experiences plastic deformation. In the graph below, the stresses for the three different pipes are shown and it can be noticed that the pipe A, having the smallest of the holes, reaches the yield stress with a lower applied torque than pipe C, which has the largest hole. A path along the nodes at the holes was drawn to record the stresses around it at a normal distance from the node point: therefore a sinusoidal curve was found, and, for the symmetrical arrangement of the stresses, only a quarter of the path has been exported in the graph below. The horizontal line on the top represents the yield stress, until which the material will behave linearly.

The reason behind this behaviour is to be found in the elastic region of the metal. A large hole, as shown in the Figure above, would dissipate the stresses in large areas and therefore yield with higher applied rotation, while smaller holes concentrate the stresses around the cut-out in a smaller area. This is also seen in the fact that cylinders with larger holes tend to be more flexible and therefore accumulate smaller stresses when loads are applied.

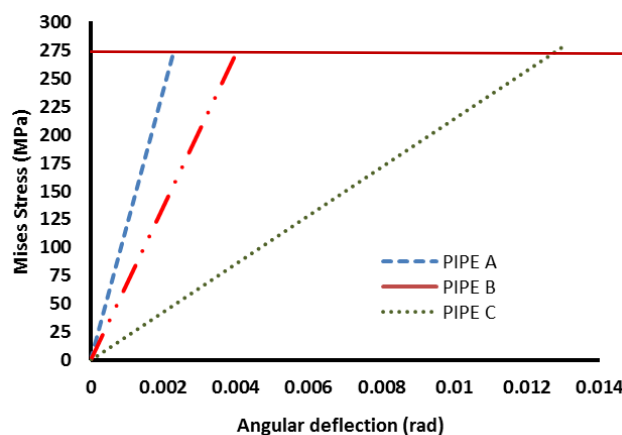


Fig. 8. The result of Mises stress versus torque applied to the pipes

The contour legend for Figures 9, 10 and 11 is chromatically distributed having the lowest stress concentration all along the pipe and the highest value recorded around the holes.

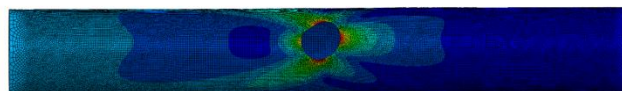


Fig. 9. Stress concentration when torsional force is applied to the pipe A

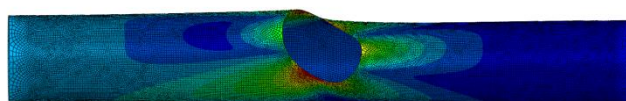


Fig. 10. Stress concentration when torsional force is applied to the pipe B

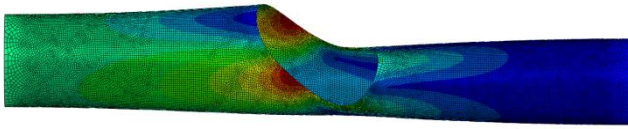


Fig. 11. Stress concentration when torsional force is applied to the pipe C

IV. CONCLUSION

As a conclusion, it can be said that the results of current studies generally agree with the previous work done by Bull [5] on stresses around large circular holes in uniform circular cylinders. It can also be seen that the larger the hole, the greater the reduction in stiffness, as shown in Figure 8. A larger angular deflection is required for Pipe C to achieve the same stresses in Pipe A, therefore there is a reduction in torsional resistance. As well as this, the larger the hole the higher the stress concentration values under equivalent loading. This can be seen in the compressive stress analyses, with Pipe C achieving the largest stress values for the three pipes under identical compressive force.

ACKNOWLEDGMENT

The authors' thank the Civil Engineering Department at Brunel University London for supporting this paper and for their constant encouragement throughout the work.

REFERENCES

- [1] Ventsel E., Krauthammer T., (2001), "Thin Plates and Shells – Theory, Analysis, and Application", Marcel Dekker, Inc. New York, Basel.
- [2] Gibson J. E., (1965) "Linear elastic theory of thin shells", Pergamon Press
- [3] Naghdi A. K., Eringen A. G., "Stress distribution in a circular cylindrical shell with circular cut-out", *Archive of Applied Mechanics*, 34(3), pp.161-172.
- [4] Lianga C.C., Hsu C. Y., Chen W., (1998), "Curvature effects on stress concentration around circular holes in opened shallow cylindrical shell under external loading", *International Journal of Pressure Vessel and Piping*, 75, pp. 749-763.
- [5] Bull J. W., (1982), "Stress around large circular holes in uniform circular cylinder", *The Journal of Strain Analysis for Engineering Design*, 17, pp. 9-12.
- [6] Troyani N., Pérez A., Baíz P., (2005), "Effect of finite element mesh orientation on solution accuracy for torsional problems", *Finite Elements in Analysis and Design*, 41, pp. 1377–1383.
- [7] Sadowski A. J., Rotter M. J, (2013), "On the relationship between mesh and stress field orientations in linear stability analyses of thin plates and shells", *Finite Elements In Analysis And Design*, 73, pp. 42-54, ISSN: 0168-874X.